Crossed ratchet effects for magnetic domain wall motion

A. Pérez-Junquera,[1] V. I. Marconi,[2] A. B. Kolton,[2] L. M. Álvarez-Prado,[1] Y. Souche,[3] A. Alija,[1] M. Vélez,[1,*] J. V. Anguita,[4] J. M. Alameda,[1] J. I. Martín,[1] and J. M. R. Parrondo[2]

[1] *Depto. Física, Universidad de Oviedo, 33007 Oviedo, Spain*
[2] *Depto. Física Atómica, Molecular y Nuclear, and* GISC, *Universidad Complutense de Madrid, 28040 Madrid, Spain*
[3] *Institut Néel, CNRS/UJF, BP 166, 38042 Grenoble, France*
[4] *Instituto de Microlectrónica de Madrid (CNM-CSIC), Tres Cantos, 28760 Madrid, Spain*

We study both experimentally and theoretically the driven motion of domain walls in extended amorphous magnetic films patterned with a periodic array of asymmetric holes. We find two crossed ratchet effects of opposite sign that change the preferred sense for domain wall propagation, depending on whether a flat or a kinked wall is moving. By solving numerically a simple ϕ^4-model we show that the essential physical ingredients for this effect are quite generic and could be realized in other experimental systems involving elastic interfaces moving in multidimensional ratchet potentials.

PACS numbers: 75.60.Ej, 75.60.Ch, 74.25.Qt

The propagation of domain walls in thin ferromagnetic films is a problem of great current interest. It provides both the basis for a wide number of modern magnetic devices [1] and an excellent experimental system to study the basic physics of an elastic interface in the presence of either ordered or random pinning defects [2, 3, 4, 5, 6]. Such physics has been indeed recently considered in many other experimental systems involving interfaces, such as ferroelectric domain walls [7], contact lines of liquids menisci [8] or fractures [9]. Furthermore, it is relevant for systems involving periodic elastic manifolds, such as vortex lattices in superconductors [10], charge density waves [11] or Wigner crystals [12].

A case of particular interest appears when the pinning potential is asymmetric, favoring the propagation of the elastic interface in one direction. This gives rise to several ratchet effects [13], which are a potential tool to control motion at micro and nanoscales in a variety of systems [14]. One of the first known examples of ratchet potentials in the field of magnetism is the use of "angelfish" patterns for controlling the sense of propagation of bubble domains in domain shift registers [15]. Much more recently, the asymmetric motion of domain walls (DWs) in nanowires with a triangular structure [16] or with a set of asymmetric notches [17, 18] has also been reported. In all previous cases, domain wall propagation is restricted to a narrow 1D path (either by narrow guide rails or by the nanowire geometry) and its transverse wandering can be neglected. Then the wall behaves essentially as a point particle in a 1D asymmetric potential, provided effectively by the 2D geometry of the patterned film. However, in a thin extended film, a DW is an elastic line that can distort all along its length in response to the 2D asymmetric pinning potential. The competition between elasticity and pinning is a purely collective behavior and can thus yield novel ratchet phenomena.

In this work, we study the propagation of DWs in *extended* amorphous magnetic films patterned with a periodic array of asymmetric holes. We observe experimentally, for the first time, two crossed ratchet effects of opposite sign that change the preferred sense for DW motion depending on whether a flat or a kinked wall is moving. By identifying the essential physics we show that this effect could be realized in other *multidimensional* ratchet systems involving the motion of elastic interfaces.

Amorphous 40 nm thick magnetic Co-Si films have been fabricated by sputtering with a well defined uniaxial anisotropy and a low coercivity [19]. In these films, easy axis (EA) magnetization reversal takes place by propagation of 180° Néel walls that tend to lie parallel to the EA [20]. A $500 \times 500\,\mu\text{m}^2$ ordered array of asymmetric antidots has been patterned by a combination of e-beam lithography and an Ar^+ etching process [21]. Each hole is shaped as a small arrow pointing perpendicular to the uniaxial EA (see Fig. 1(a)). This allows us to define two different senses of propagation for a DW lying along the EA (Y axis): "forward" ($\mathcal{F}$), from left to right, i.e towards the direction pointed by the arrows, and "backward" ($\mathcal{B}$), from right to left. The asymmetric antidots are arranged in a square array parallel to the EA, with a $20 \times 20\,\mu\text{m}^2$ unit cell, centered in a $500\,\mu$m wide path and separated from the rest of the film by a $5\,\mu$m wide trench. Magnetic properties have been characterized both by Transverse Magnetooptical Kerr effect (MOKE), using a setup with a laser focused in a $300\,\mu$m spot in the desired sample area [20], and by MOKE microscopy [22]. The magnetic field, H, is applied parallel to the film plane and along the EA.

In Fig. 1(b) we show hysteresis loops measured both at the array area (circles) and at the unpatterned regions in the left (triangles) and in the right (squares) sides of the array. The observed increment in coercive field (H_C) from 6.5 Oe in the continuous film to 8.6 Oe in the array is a clear evidence that the fabricated holes act as effective pinning centers, useful to control the DW motion. This difference in coercivity implies that there is a field

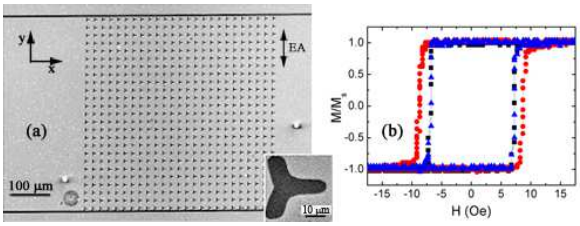

FIG. 1: (color online) (a) Scanning electron microscopy image of an array of asymmetric holes. Inset shows a detail of a single arrow hole. The easy axis direction is also indicated. (b) MOKE hysteresis loop measured at the array (circles) and at the unpatterned regions at the right (squares) and at the left (triangles) of the array.

range, approximately between 6.5 Oe and 8 Oe, where the continuous regions have been reversed but not the patterned area, which will be bounded by two DWs at its left and right sides. This is indeed observed in the Kerr microscopy images shown in Figs.2(a-b) taken at $H = 8\,$Oe after saturating the sample with a large negative field. A DW can be identified in each image as the line separating the dark-clear contrast regions (i.e. negative and positive magnetization). The walls are located either at the first (Fig. 2(a)) or at the last (Fig. 2(b)) column of defects, indicating that they cannot move further inside the array area due to the antidot pinning. Upon further increasing the applied field to $H = 8.4\,$Oe, the left wall penetrates the array, (see Fig. 2(c), in which the left wall is pinned between the 4^{th} and 5^{th} antidot columns). Then, at $H = 8.8\,$Oe, it can be seen in Fig. 2(d) that the left wall has propagated in the $\mathcal{F}$ direction, now up to the 17^{th} defect column, whereas the right wall has not been yet able to move. Finally, for larger fields, both walls coalesce completing the magnetization reversal at the array area (Fig. 2(e)). This reversal sequence clearly shows that the depinning field for $\mathcal{F}$ wall propagation $H_{\mathcal{F}} \approx 8.4\,$Oe is lower than the field for $\mathcal{B}$ wall depinning $H_{\mathcal{B}} \geq 8.8\,$Oe (only a lower bound can be obtained in this case) indicating that the arrow-shaped holes act as asymmetric pinning centers for the DWs. A similar image sequence for the descending field branch in the hysteresis loops shows again a wall entering from the left and moving in the $\mathcal{F}$ direction, only with an overall exchange between the black/white contrast regions (i.e an overall magnetization sign change). It is important to note that the easy direction of motion in the patterned area is that in which the length of the pinned wall between two antidots increases smoothly, in agreement with the reported behavior in nanowires of triangular cross section [16, 17].

To study the motion of a single DW inside the array, the following experiment has been performed (see the field *vs.* time sequence $H(t)$ in Fig. 3(a)): after a first complete major loop between $t = 0$ and $t = 0.25$ s, the sample is saturated in a large negative field. Next, the field is increased up to the positive coercivity, where a single DW enters in the middle of the array and, then, H is decreased. Finally, at $t = t_0$, a triangular field ramp

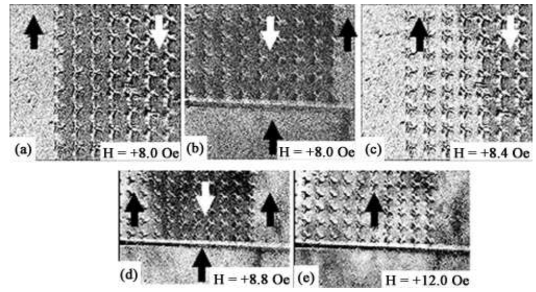

FIG. 2: (a)-(e) Sequence of MOKE microscopy images taken in the ascending field branch of the hysteresis loop after saturation in a negative field.

of increasing amplitude H_{max} is applied to the sample. The corresponding time evolution of the magnetization is shown at the bottom of Fig. 3(a), both in the patterned and unpatterned regions. Surprisingly, during several field cycles (between t_0 and t_1), there is a net *decrease* in the magnetization of the array (see inset of Fig. 3(a)), indicating $\mathcal{B}$ DW motion. The sign of the $\partial M/\partial t$ slope at $t = t_0$ is found to depend only on the sign of the saturation magnetization M_S before introducing the wall inside the array, and not on the sign of $\partial H/\partial t$, as would be in a standard accommodation effect [23]. Fig. 3(b) shows several stable minor loops, measured with a similar $H(t)$ sequence as in Fig. 3(a), but with a constant amplitude $H_{max} < 8\,$Oe in the triangular ramp after t_0 and centered along the magnetization axis. These minor loops exhibit a clear asymmetry, quantified by the difference between the positive and negative coercivities $\Delta H_C = H_C^{asc} - H_C^{desc}$ of about 0.2 Oe (Fig. 3(c)). Different from exchange bias, the sign of ΔH_C is found to depend on the sign of M_S before introducing the wall, so that coercivity is always lower when the wall is pushed in the $\mathcal{B}$ direction.

From these data, two main results are worth remarking: first, the system "keeps memory" of the last saturating state that can be read in the sign of ΔH_C or of $\partial M/\partial t$ at $t = t_0$. Second, there is a clear change between the behavior observed in Fig. 2, in which the DW penetrates into the array more easily in the $\mathcal{F}$ direction, and the minor loop experiment of Fig. 3, in which DW motion within the array is easier in the $\mathcal{B}$ direction.

To understand these opposite effects, a crucial observation is the change in the wall configuration as it enters the array: in the continuous area, the wall is essentially flat (Fig. 2(a-b)) but it develops kinks when it is pinned into the array (Fig. 2(c)). This suggests an extra mechanism for DW motion in the minor loop experiment, through upward/downward ($\mathcal{U}/\mathcal{D}$) kink propagation, that is possible in our geometry but not in the

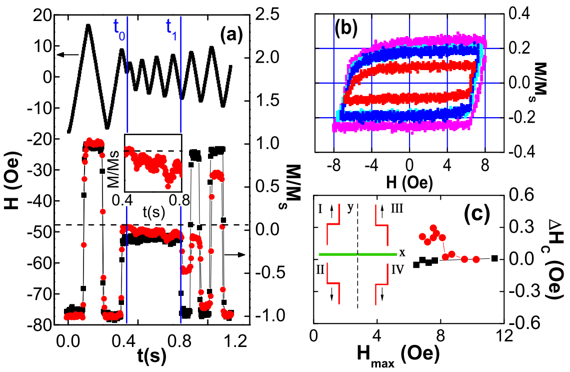

FIG. 3: (color online) (a) $H(t)$ sequence used to introduce a wall inside the array and measure its propagation within it (top); corresponding $M(t)$ response in the array (red circles) and in the continuous film (black squares). Inset shows a zoom of the decrease in magnetization from t_0 to t_1 in the array. (b) Minor hysteresis loops measured after introducing a wall inside the array at the positive coercivity. (c) Coercive field asymmetry as a function of minor loop amplitude in the array (red symbols) and in the unpatterned area (black symbols). Inset shows the results of X axis reflection and Y axis reflection (broken symmetry in the array) on a kink moving upward.

more restricted nanowire case where the DW can not develop kinks. Indeed, by taking into account the reflection symmetries of the array as depicted in the inset of Fig. 3(c), it is easy to see that a kink propagating $\mathcal{U}$ (I) would be equivalent to an antikink propagating $\mathcal{D}$ (II) but not necessarily equivalent to a kink propagating $\mathcal{D}$ (IV) or to an antikink propagating $\mathcal{U}$ (III) (see also the insets in Fig. 4). Therefore, the array could in principle induce an *asymmetric pinning for kink motion*, i.e. perpendicular to the previously described ratchet affecting the $\mathcal{F}/\mathcal{B}$ propagation of the flat wall. Most interestingly, the experimental results of Figs. 2 and 3 suggest that these *crossed ratchet effects* must be of opposite sign.

To check the above scenario we consider the competition between drive, elasticity and the asymmetric pinning on a single driven DW. For this purpose we simulated the paradigmatic ϕ^4-model for a scalar order parameter $\phi(x, y; t)$, in which a DW provides a smooth transition between energetically equivalent minima of a simple free energy [24]. We will show that this approach, although simplistic as it avoids many of the complications of the full micromagnetic model, has the main physical ingredients for the effect, and most importantly, allows us to demonstrate the general nature of the observed ratchet phenomena. In our model $\phi(x, y; t)$ can be thought as a projection of the coarse-grained magnetization vector along the easy direction. We consider the evolution of ϕ in the domain $\Omega - \triangle$, which includes all the space Ω, except the region $\triangle$ occupied by antidots. In order to model the absence of magnetic material in $\triangle$, we set Neumann boundary conditions $\partial_{\mathbf{n}}\phi|_{\partial\triangle} = 0$ at the antidot borders $\partial\triangle$. Finally, considering a purely dissipative dynamics, the equation of motion for ϕ can be written as [24]

$$\eta \partial_t \phi = c\nabla^2\phi + \epsilon_0\Big(\phi - \phi^3\Big) + H \qquad (1)$$

where c is the elastic stiffness of the order parameter, ϵ_0 is proportional to the local barrier separating the two equivalent minima of the free energy density, H represents the magnetic field, and the friction coefficient η sets the microscopic time-scale. The relevant parameters c and ϵ_0 will determine both the width $\xi \propto \sqrt{c/\epsilon_0}$ and the line tension $\sigma \propto \sqrt{c\epsilon_0}$ of the DW [24].

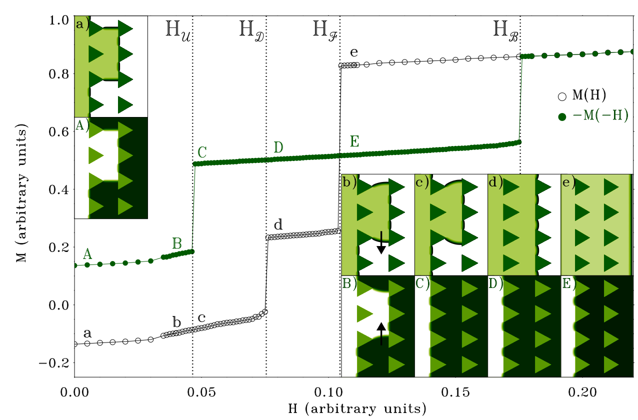

FIG. 4: (color online) Numerical results for the magnetic response of a kinked domain wall vs applied magnetic field. The initial state at $H = 0$ is a wall with a kink-antikink pair (insets a) and A)), which evolves asymmetrically with respect to H and $-H$. Insets are snapshots of the local magnetization ϕ, for different pairs of fields of equal magnitude, marked in the magnetization curves as a,...e, in $M(H)$, and as A,...E in $-M(-H)$. Critical fields show clearly that it is easier to move a flat wall to the right than to the left but on the contrary the kinked wall is harder to move to the right than to the left.

For the simulation we chose $\epsilon_0 = \eta = 1$ and c such that ξ is 10% of the characteristic size of the antidots, which approximately corresponds to the realistic situation [20], although we obtain qualitatively the same behavior for a finite range of parameters. We solve numerically the Eq. (1) in a $L_x \times L_y$ box with periodic boundary conditions in the Y direction, and model the asymmetrical antidots as a rectangular array of triangular holes pointing to the positive X direction (see insets in Fig. 4). To ensure the presence of a DW along the sample, we set $\phi(x = 0, y; t) = 1$ and $\phi(x = L_x, y; t) = -1$ as boundary conditions in the X direction, and then probe the response of the DW to different, positive and negative magnetic fields H. Since we are interested in the response to constant or low-frequency fields, we will only analyze the stationary magnetization $M(H)$, starting with the particular initial condition of a single flat DW with a kink-antikink pair (see insets A and a in Fig. 4).

In Fig. 4 we show the magnetization M vs the applied magnetic field H starting at $H = 0$ with the kink-antikink pair [25]. As indicated by the vertical dotted-lines we can clearly distinguish four critical fields: $H_{\mathcal{U}}$ corresponds to the $\mathcal{U}$ ($\mathcal{D}$) depinning of a kink (antikink), cases I and II in Fig. 3(c), which amounts to a net motion of our initial DW to the left ($\mathcal{B}$); $H_{\mathcal{D}}$ is the depinning field for the $\mathcal{D}$ ($\mathcal{U}$) motion of a kink (antikink), cases IV and III in Fig. 3(c); $H_{\mathcal{F}}$ and $H_{\mathcal{B}}$ corresponding to the $\mathcal{F}$ and $\mathcal{B}$ depinning fields of flat walls, respectively. We find that $H_{\mathcal{U}} < H_{\mathcal{D}} < H_{\mathcal{F}} < H_{\mathcal{B}}$. As expected, transport at low fields $|H| < H_{\mathcal{F}}$ is dominated by the presence of mobile kinks. More interestingly, we have $H_{\mathcal{U}} < H_{\mathcal{D}}$. This implies that a net directed transport of the wall in the $\mathcal{B}$ direction can be obtained under an low-frequency ac-field of amplitude $H_{\mathcal{U}} < |H| < H_{\mathcal{D}}$, in qualitative agreement with the behavior of the magnetization in the minor loop experiment, between t_0 and t_1 shown in Fig. 3(a). Finally, by increasing the magnetic field amplitude $|H|$ we have an inversion of the rectification for flat walls, since $H_{\mathcal{B}} > H_{\mathcal{F}}$, i.e., the wall as a whole moves more easily in the $\mathcal{F}$ direction, as in the experiments (cf. Fig. 2). The simulations also show which are the key ingredients for the inversion in the rectification between these two crossed ratchet effects: whereas the $\mathcal{B}$ motion of a flat wall (Fig. 4 inset E) involves a sudden (i.e. long-range correlated) depinning from the stable position at the base of the triangles, making it the *hard* direction of motion, the $\mathcal{B}$ motion of a kinked wall involves the $\mathcal{U}$ motion of a kink (Fig. 4 inset B), which gradually peels off the wall from the triangle bases thus making this, on the contrary, the *easy* direction of motion for a kinked wall at low fields. It is worth noting that this behaviour is due to the generic interplay between elasticity, pinning, and drive: while the first two tend to minimize the line energy of the DW by respectively straightening all segments and by optimally using the holes bridging them, the applied field tends to increase the area behind the DW with $\phi H > 0$. This leads to the characteristic catenary shape of all pinned segments and finally to the asymmetric depinning configurations and forces, responsible for the observed ratchet effects.

In summary, our experimental and theoretical study of the DW propagation across an array of asymmetric holes has revealed the existence of two crossed ratchet effects: the first one favors $\mathcal{F}$ motion of a flat wall while the second acts on the $\mathcal{U}/\mathcal{D}$ kink propagation favoring net $\mathcal{B}$ wall motion at low fields. As a result of the interplay between both ratchets, the system keeps memory of the sign of the last saturating state even in a zero magnetization configuration, thus opening an interesting possibility for future applications in memory devices. It is worth noting that this effect relies completely in the extended nature of the DW, which allows excitations transverse to the direction of propagation. Moreover, the identification of the main physical ingredients for this novel effect shows that it could be realized in other experimental systems involving the motion of elastic interfaces or domain walls in multidimensional ratchet potentials.

Work supported by Spanish CICYT under grants NAN2004-09087, MOSAICO, and FIS2005-07392. We acknowledge helpful discussions with Prof. J.L. Vicent.

* Electronic address: mvelez@uniovi.es

[1] C. D. Mee and E. D. Daniel, Magnetic Storage Handbook(1996) (New York: McGraw-Hill); G. Prinz, J. Magn. Magn. Mater. **200**, 57 (1999).
[2] M. Kardar, cond-mat/9704172; T. Giamarchi, A. B. Kolton, A. Rosso, in *Jamming, Yielding, and Irreversible Deformation in Condensed Matter*, edited by M.C. Miguel and J.M. Rubi, Lecture Notes in Physics **688**, 91 (2006) (Springer).
[3] S. Lemerle *et al.*, Phys. Rev. Lett. **80** 849 (1998).
[4] J. P. Attane *et al.*, Phys. Rev. Lett. **93**, 257203 (2004).
[5] Y. L. Iunin *et al.*, Phys. Rev. Lett. **98**, 117204 (2007).
[6] E. Martinez *et al.* Phys. Rev. Lett. **98**, 267202 (2007).
[7] P. Paruch, T. Giamarchi and J. M. Triscone, Phys. Rev. Lett. **94** 197601 (2005)
[8] S. Moulinet *et al.*,Phys. Rev. E **69** 35103 (R) (2004).
[9] L. Ponson, D. Bonamy, and E. Bouchaud, Phys. Rev. Lett. **96**, 035506 (2006).
[10] G. Blatter *et al.*, Rev. Mod. Phys. **66**, 1125 (1994).
[11] T. Nattermann and S. Brazovskii, Adv. Phys. **53** 177 (2004).
[12] T. Giamarchi, *Electronic Glasses* (Bologna: IOS Press) (2004). cond-mat/0403531.
[13] P. Reimann, Phys. Rep. **361**,57 (2002); R. D. Astumian and P. Hänggi, Physics Today **55**, 33 (2002).
[14] J. E. Villegas *et al.*, Science **302**, 1188 (2003); H. Linke *et al.*, Science **286**, 2314 (2003); D.E. Shalóm and H. Pastoriza, Phys. Rev. Lett. **94**, 177001 (2005); C.C. de Souza Silva *et al.*, Nature **440**, 651 (2006).
[15] N. Hayashi *et al.*, IEEE Trans. on Magn. **8** 370 (1972).
[16] D. A. Allwood, G. Xiong and R. P. Cowburn, Appl. Phys. Lett. **85**, 2849, (2004).
[17] A. Himeno *el. al*, J. Appl. Phys. **97**, 066101 (2005); A. Himeno, S. Kasai and T. Ono, Appl. Phys. Lett. **87**, 243108 (2005).
[18] S. Savel'ev, A. Rakhmanov and F. Nori, New J. Phys. **7**, 82 (2005).
[19] M. Vélez *et al.*, Eur. Phys. J. B **41**, 517 (2004).
[20] A. Pérez-Junquera *et al.*, J. Appl. Phys. **99**, 033902 (2006).
[21] A. Pérez-Junquera *et al.*, Nanotechnology **15**, S131 (2004).
[22] P. Molho *et al.*, J. Appl. Phys. **61**, 4188 (1987).
[23] P. J. Thompson and R. Street, J. Phys. D: Appl. Phys. **30**, 1273 (1997).
[24] See for instance, P.M.Chaikin and T.C.Lubensky, *Principles of Cond. Matter Physics* (Cambridge, 1995).
[25] See EPAPS Document No. for movies of kinked and flat DW motion at fixed magnetic fields.